A MECHANISTIC MODEL TO PREDICT FUEL CHANNEL FAILURE IN THE EVENT OF PRESSURE TUBE OVERHEATING

A.R. Dion[1], J.C. Luxat[2]
[1, 2] McMaster University, Hamilton, Ontario, Canada
luxatj@mcmaster.ca, dionar@mcmaster.ca

Abstract

Under normal operating conditions a pressure tube (PT) in the CANDU reactor is insulated from its outer calandria tube (CT) by a CO_2 gas annulus. If the primary loop coolant flow is compromised the PT can overheat and, if still pressurized, balloon into contact with the CT. At this point the moderator acts as an emergency heat sink. If the heat transferred from the CT to the moderator exceeds the critical heat flux (CHF) the CT can overheat, begin to strain due to the contact pressure, and eventually cause fuel channel failure. A mechanistic model is presented that describes ballooning contact of the PT and CT, the resulting thermal contact conductance, heat flux to the moderator, and, if CHF is exceeded, the development of film boiling and potential CT strain. The goal is to create a software package that predicts fuel channel failure during a pressure tube overheat event.

1. Introduction

The CANDU primary coolant loop consists of 380 (or 480 depending on reactor design) 4 mm thick, 10.34 cm inner diameter pressure tubes (PT) constructed of zirconium-2.5 wt% niobium. Each 6 meter length of tube passing through the reactor contains 12 natural uranium fuel bundles which, at full power, heat the coolant to temperatures upwards of 300^{o}C. To keep in loop boiling to a minimum coolant pressure is held at roughly 10 MPa. To minimize heat loss from the coolant to the moderator each PT is contained within a 1.4 mm thick 12.92 cm inner diameter calandria tube (CT) fabricated from Zircaloy-2. Under normal operating conditions the PT is insulated from the CT by a CO_2 gas annulus. In the event of loss of coolant, or reduced coolant flow, heat removal from the fuel channel will be compromised. In severe cases this can lead to PT overheating and ballooning (under pressurized conditions) or sagging (at depressurized conditions) contact with the CT. At this point the moderator acts as an emergency heat sink. If heat transfer between the CT and the moderator exceeds the critical heat flux (CHF) heat transfer between the CT and the moderator will be compromised. The CT will begin to overheat and, under sustained film boiling with sufficiently high stress and temperature, can strain to failure. The following text reviews the processes involved in PT overheat and ballooning CT contact and reports results obtained from a mechanistic model developed in MATLAB simulating these processes in an attempt to predict fuel channel failure in the event of a station blackout.

2. Governing equations of fuel channel thermal and mechanical behaviour

This section provides all relevant information and sources used in the calculation of PT/CT heat transfer and mechanical strain including the estimation of contact conductance, contact pressure, tube failure criteria, development of film boiling and possible CT quench.

The following assumptions are made during the simulation:

- Uniform PT/CT circumferential temperature.
- Heat transfer to the end caps of the apparatus is negligible.
- Pre-Contact: the heat transfer between the PT and CT that would arise through radiation and conduction through the CO_2 annulus is negligible.
- PT (and CT after contact) will maintain circular geometry during deformation.
- PT/CT remain in contact once outer PT diameter reaches the inner CT diameter.
- Post-Contact: the convective heat transfer from the CT to the moderator is uniform around the circumference.

2.1 Heat transfer equations

2.1.1 Pre-Contact

Before pressure tube and calandria tube contact we consider only the heat transferred between the fuel bundles and the pressure tube. The experimental results [1] used to validate the model, outlined later in section 3, placed a graphite electric heater inside of a void section of PT; for this reason we only consider radiation heat transfer from the heater to the PT.

$$m'_h c_{ph} \frac{dT_h}{dt} = q'_h - h'_h\left(T_h - T_{pt}\right) - \gamma' q'_h \tag{1}$$

$$m'_{pt} c_{ppt} \frac{dT_{pt}}{dt} = h'_h\left(T_h - T_{pt}\right) - q'_{loss} \tag{2}$$

The rate of change in energy stored in either the heater or pressure tube (subscripts h and pt respectively) over time is equal to the product of mass per unit length (m'), specific heat capacity (c_p) and temperature change (T) with time (t) of the component in question. For the heater this power is equal to the power produced by the heater (q'_h) minus the heat transferred to the PT based on the radiation heat transfer coefficient (${h_h}'$) and losses ($\gamma' q'_h$). For the purposes of this simulation γ'=0. The radiation heat transfer coefficient is a function of heater and inner (i) pressure tube diameters (D), emissivities (ϵ) and temperatures. For the heat transferred from the heater to the PT:

$$h'_h = \frac{\pi\sigma(D_h\epsilon_h)\left(D_{pti}\epsilon_{pt}\right)\left(T_h^2 + T_{pt}^2\right)\left(T_h + T_{pt}\right)}{(D_h\epsilon_h)\left(1 - \epsilon_{pt}\right) + (D_{pti}\epsilon_{pt})} \tag{3}$$

q'_{loss} is the fraction of heat lost from the PT which is assumed to be negligible before contact.

2.1.2 Post-Contact

After contact equation 2 is modified by replacing q'_{loss} by the heat transfer from the PT to the CT. We must also consider the heat transferred from the CT to the moderator.

$$m'_{pt} c_{ppt} \frac{dT_{pt}}{dt} = q'_{pt} - h'eff(T_{pt} - T_c) \tag{4}$$

$$m'_{ct} c_{pct} \frac{dT_{ct}}{dt} = h'_{eff}(T_{pt} - T_{ct}) - h'_{conv}(T_{ct} - T_l) \tag{5}$$

The heat transfer coefficient (h'_{eff}) between the tubes depends on the thermal contact conductance (h_c), thickness (τ), conductivity (k) and diameter of the contacting tubes.

$$h'_{eff} = \left(\frac{\tau_{pt} D_{cti}}{k_{pt} D_{pt}} + \frac{D_{cti}}{h_c D_{pt}} + \frac{\tau_{ct}}{k_{ct}} \right)^{-1} \tag{6}$$

The total energy change over time in the CT is the difference between the heat transferred to the CT from the PT and the heat rejected to the moderator which will be determined by the convective heat transfer coefficient (h'_{conv}). Under nucleate boiling conditions h'_{conv} takes a value in the range of 10-50 kW/m^2/K. In film boiling conditions this value can drop to the order of 1 kW/m^2/K depending on the bulk moderator temperature (T_l) [2]. A more in depth description of the convective heat transfer coefficient will be discussed in section 2.5.

2.2 PT & CT strain

Shewfelt et al. [3] performed experiments on zirconium-2.5 wt% niobium (Zr-2.5%Nb) test sections cut from pressure tubes in the transverse and longitudinal directions. Using resistive heating and a hydraulic testing machine samples were tested a heatup rates of 50^{o}C/s to determine the transverse stress (σ_{pt}) and strain temperature dependence. At temperatures between 450^{o}C and 850^{o}C the dominant modes of strain were the power-law creep in the α-phase ($\dot{\epsilon}_a$) and the grain boundary sliding ($\dot{\epsilon}_{gb}$).

$$\dot{\epsilon}_{pt} = \dot{\epsilon_\alpha} + \dot{\epsilon}_{gb} \tag{7}$$

$$\dot{\epsilon}_{pt} = 1.3\times10^{-5} \sigma_{pt}^9 \exp\left(-\frac{36600}{T_{pt}}\right) + \frac{5.7\times10^7 \sigma_{pt}^{1.8} \exp\left(-\frac{29200}{T_{pt}}\right)}{\left[1 + 2\times10^{10} \int_{t_1}^{t} \exp\left(-\frac{29200}{T_{pt}}\right) dt\right]^{0.42}} \tag{8}$$

The strain hardening integral in the denominator is evaluated from the time (t_1) at which the sample temperature reached 700^{o}C. At temperatures above 850^{o}C up to 1200^{o}C the strain is dominated by the grain boundary sliding and the β-phase power-law creep ($\dot{\epsilon}_\beta$).

$$\dot{\epsilon}_{pt} = \dot{\epsilon}_\beta + \dot{\epsilon}_{gb} \tag{9}$$

$$\dot{\epsilon}_{pt} = 10.4 \sigma_{pt}^{3.3} \exp\left(-\frac{19600}{T_{pt}}\right) + \frac{3.5\times10^4 \sigma_{pt}^{1.4} \exp\left(-\frac{19600}{T_{pt}}\right)}{1 + 274 \int_{t_2}^{t} \exp\left(-\frac{19600}{T_{pt}}\right) \left(T_{pt} - 1105\right)^{3.72} dt} \tag{10}$$

In this case the strain hardening integral is evaluated from the time (t_2) at which the sample reached 850^{o}C. This study was repeated for Zircaloy-2 test sections [4] cut from calandria tubes. The study showed that the total transverse creep was the sum of the dislocation creep ($\dot{\epsilon}_d$) and grain boundary sliding and was dependent on the transverse stress (σ_{ct}), temperature and the internal stress in the α-phase (σ_i).

$$\dot{\epsilon}_{ct} = \dot{\epsilon}_d + \dot{\epsilon}_{gb} \tag{11}$$

$$\dot{\epsilon}_{ct} = 22000(\sigma_{ct} - \sigma_i)^{5.1} \exp\left(-\frac{34500}{T_{ct}}\right) + 140\sigma_{ct}^{1.3} \exp\left(-\frac{19000}{T_{ct}}\right) \tag{12}$$

$$\sigma_i = 1.4 + \int_0^t \left[110\dot{\epsilon}_d - 3.5\times10^{10}\sigma_i^{1.8} \exp\left(-\frac{34500}{T_{ct}}\right)\right] dt \tag{13}$$

Since the $\dot{\epsilon}_d$ is dependent on σ_i, which is itself dependent on $\dot{\epsilon}_d$, an iterative method is used to solve for the CT strain rate. A guess at the value of σ_i is made and it is used to evaluate $\dot{\epsilon}_d$ which is then used to reevaluate σ_i. The value of σ_i is accepted once the evaluated value converges within 0.1% of the initial guess. Once the strain rate has been calculated for either tube it is multiplied by the time step used in the simulation to obtain the strain. The change in radius and thickness of either the PT or CT is described by:

$$r_f = r_i(1 + \epsilon) \tag{14}$$

$$\tau_f = \tau_i/(1 + \epsilon) \tag{15}$$

Where the subscript f indicates the radius (r) and thickness (τ) that the tube in question has crept to from its original size i for the current time step.

2.3 Thermal contact conductance

The thermal contact conductance is calculated based on the method proposed by Yovanovich [5]. This model considers the thermal conductance of two solids that sandwich some interstitial fluid between the asperities forming the solid contact interface. The total conductance is written as:

$$h_c = h_s + h_g \tag{16}$$

Solid contact conductance (h_s) is dependent of the effective root mean square total (RMS) of asperity slopes (m), RMS roughness (σ_{rms}), harmonic mean of conductivities (k_s) and the ratio of contact pressure (P) to material hardness (H).

$$h_s = \frac{1.25mk_s}{\sigma_{rms}} \left(\frac{P}{H}\right)^{0.95} \tag{17}$$

Material hardness is determined by selecting the softer of the two interfacing solids' Meyer hardness value (in Pa)

$$H = \exp\left(26.034 - 2.639\times10^{-2}T + 4.3504\times10^{-5}T^2 - 2.561\times10^{-8}T^3\right) \tag{18}$$

Fluid conduction will depend on fluid conductivity (k_{go}), average distance between the solids (Y), a fluid parameter (β), the mean free path of the gas (Λ) and an accommodation parameter (α):

$$h_g = \frac{k_{go}}{Y + \alpha\beta\Lambda} \tag{19}$$

Gas gaps form because of imperfections on the surface of the contacting material so the average gas gap is assumed to be dependent on the roughness of the both solid surfaces and the contacting pressure. Yovanovich provides a correlations for Y:

$$Y = 1.184\sigma\left(-\ln\left(\frac{3.132P}{H}\right)\right)^{0.547} \tag{20}$$

The fluid parameter is a function of the heat capacity ratio ($\gamma = c_p/c_v$) and the Prandtl (Pr) number for the trapped gas.

$$\beta = \frac{2\gamma}{\gamma + 1}\frac{1}{Pr} \tag{21}$$

Λ depends on a reference mean free path at a specified temperature (T_o) and pressure (P_o).

$$\Lambda = \Lambda_o \frac{T}{T_o}\frac{P_{go}}{P_g} \tag{22}$$

The accommodation parameter consists of several properties including microgeometry, gas and solid molecular weight, and surface contaminants and was described by Shlykov [6] as:

$$\alpha_n = \exp\left[-0.57\left(\frac{T_n - T_o}{T_o}\right)\right]\left(\frac{M_g^*}{6.8 + M_g^*}\right) + \frac{2.4\mu}{1+\mu^2}\left\{1 - \exp\left[-0.57\left(\frac{T_n - T_o}{T_o}\right)\right]\right\} \tag{23}$$

The subscript (n) is used to identify which surface and gas interaction is being considered where $n = 1$ or $n = 2$ for the gas/PT and gas/CT interactions respectively. Temperatures in this case refer either to the temperature of the solid (T_n) or the reference temperature ($T_o = 273$ K). In the case of a polyatomic gas (such as CO_2) Mg^* takes on the value of 1.4 times the molecular mass of the gas and μ is the ratio of gas and solid molecular weight. After evaluating α_n for both interfaces the overall accommodation parameter is given by:

$$\alpha = \frac{2 - \alpha_1}{\alpha_1} + \frac{2 - \alpha_2}{\alpha_2} \tag{24}$$

Luxat [1] reported that contact conductance can exceed 11 kW/m^2/K at initial PT/CT contact and will decrease rapidly to about 1 kW/m^2/K within seconds. Figure 1 shows typical behaviour of the outlined thermal contact conductance calculation for quench conditions. These result were obtained using an RMS roughness and average asperity slope, at contact, of 11 μm and 0.12 respectively. Experiments done by Dai et al. [7] investigated the effect of true strain on surface roughness of aluminium and suggested a linear relationship of about 4.82 μm/strain. If the PT follows the same relationship then for contact to occur with an RMS roughness of 11 μm the initial roughness would be ~10 μm (based on 18% strain to contact). Measurements performed by Shewfelt et al. [8] when validating GRAD showed a maximum variation in wall thickness of approximately 13 μm which would agree with the prescribed average RMS roughness.

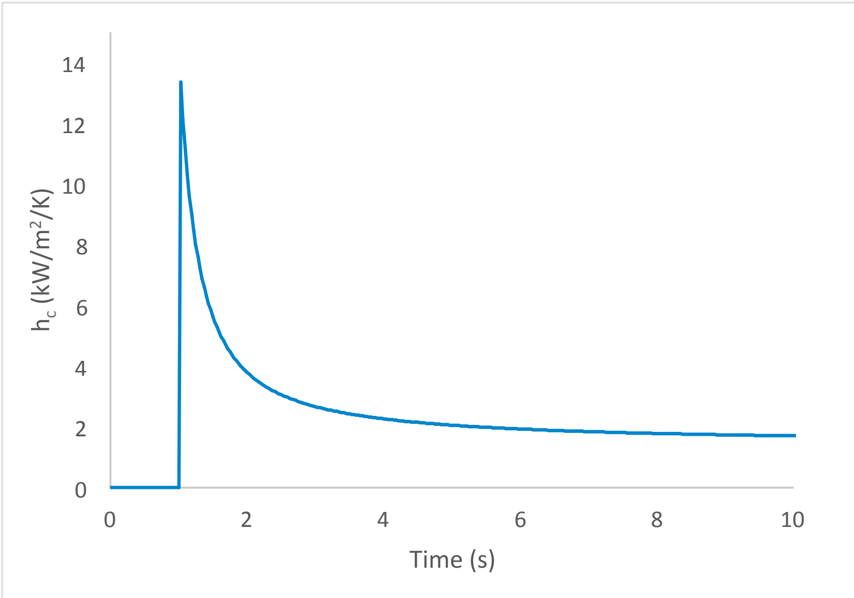

Figure 1 Thermal contact conductance ($\boldsymbol{h_c}$) as a function of time after PT/CT contact for typical quench behaviour. Note that contact occurs at 1 second for plotting purposes only. Contact time will differ with each experiment.

2.4 Contact pressure

Once the PT makes contact with the CT it is assumed that they do not separate and pressure is transferred, in part, to the CT. To determine the contact pressure we assume that, since the tubes are in contact, the strain experienced by both tubes are equal.

$$\epsilon_{pt} = \epsilon_{ct} \tag{25}$$

The transverse stress experienced by the pressure tube will be reduced by the contacting pressure and is a function of internal pressure (P_{pt}), radius (r_{pt}) and thickness.

$$\sigma_{pt} = \frac{\left(P_{pt} - P_{contact}\right) r_{pt}}{\tau_{pt}} \tag{26}$$

In a similar fashion the transverse stress experienced by the CT will increase based on the contact pressure.

$$\sigma_{ct} = \frac{(P_{contact} - P_{ext}) r_{ct}}{\tau_{ct}} \tag{27}$$

Writing the strain as the product of transverse stress with the ratio of radius and elastic modulus (E) we have:

$$\frac{\left(P_{pt} - P_{contact}\right)r_{pt}^2}{\tau_{pt}E_{pt}} = \frac{\left(P_{contact} - P_{ext}\right)r_{ct}^2}{\tau_{ct}E_{ct}} \tag{28}$$

Solving for contact pressure:

$$P_{contact} = \frac{P_{pt} + P_{ext}\phi}{\phi + 1} \tag{29}$$

$$\phi = \frac{r_{ct}^2\tau_{pt}E_{pt}}{r_{pt}^2\tau_{ct}E_{ct}} \tag{30}$$

Ronsinger et al. [9] provide correlations for Young's modulus of elasticity (in GPa) in the range of 300-1000 K for both Zr 2.5% Nb and Zircaloy-2 using the free-free resonant beam technique.

$$E = 97.05 - 0.0580(T - 273) \quad \text{Zircaloy-2} \tag{31}$$

$$E = 95.90 - 0.0572(T - 273) \quad \text{Zr 2.5\% Nb} \tag{32}$$

2.5 Boiling water heat transfer

Three regimes are considered when determining the convective heat transfer (h_{conv}) from the CT to the bulk fluid: natural convection, nucleate boiling, and film boiling. The criteria used to determine the appropriate regime, and the behaviour of h_{conv} in that regime, is described in this section. All thermodynamic properties of water were obtained using the MATLAB function XSteam developed by Holmgren [10].

2.5.1 Natural Convection

For a very brief moment, when the PT first contacts the CT, the CT temperature will be equal to the bulk fluid temperature and will increase as heat is transferred between the contacting tubes. As the CT temperature increases above the bulk temperature but remains below saturation temperature (T_{sat} = 373 K) heat transfer will be through natural convection. We can, therefore, determine the convective heat transfer coefficient [10] based on the Nusselt number ($\overline{Nu_D}$):

$$\overline{Nu_D} = \frac{h_{conv}L}{k} \tag{33}$$

Where L is the characteristic length of the system ($\pi D_{ct}/2$ for a horizontal cylinder) and k is the conductivity of the fluid (evaluated at the film temperature). The Nusselt number can also be correlated to the Rayleigh (Ra_D) and the Prandtl (Pr) number based on the condition of the boundary layer [10]:

$$\overline{Nu_D} = 0.36 + \frac{0.518 Ra_D^{\frac{1}{4}}}{\left[1 + \left(\frac{0.559}{Pr}\right)^{\frac{9}{16}}\right]^{\frac{4}{9}}} \qquad 10^{-6} < Ra_D \leq 10^9 \tag{34}$$

$$\overline{Nu_D} = \left\{0.60 + \left[\frac{0.387 Ra_D}{\left[1 + \left(\frac{0.559}{Pr}\right)^{\frac{9}{16}}\right]^{\frac{16}{9}}}\right]^{1/6}\right\}^2 \qquad Ra_D \geq 10^9 \tag{35}$$

Where

$$Ra_D = \frac{g\beta}{\nu\alpha}(T_{ct} - T_b)L^3 \tag{36}$$

$$Pr = \frac{c_p \mu}{k} \tag{37}$$

Values for kinematic viscosity (ν), thermal diffusivity (α), specific heat (c_p), dynamic viscosity (μ), and thermal expansion coefficient (β) are all evaluated at film temperature. In all simulations Ra_D was predicted to be larger than 10^9 indicating a turbulent boundary layer and thus equation 33 was used to predict h_{conv}.

2.5.2 Nucleate Boiling

Once the CT temperature rises above saturation temperature the program switches to the nucleate boiling regime. Luxat [1] reports the nucleate boiling heat transfer coefficient being between 10 and 50 kW/m^2/K. The later was chosen, as a conservative estimate, whenever the program found itself in the nucleate boiling regime.

2.5.3 Film Boiling

To enter film boiling the heat transferred from the CT to the bulk fluid must exceed the critical heat flux (CHF). Subcooled pool boiling CHF can be determined using the Ivey and Morris correction factor [11]:

$$\frac{q''_{chfsc}}{q''_{chfsat}} = 1 + 0.1\left(\frac{c_p(T_{sat} - T_b)}{h_{fg}}\right)\left(\frac{\rho_f}{\rho_l}\right)^{0.75} \tag{38}$$

Where q''_{chfsat} is the saturated pool critical heat flux which can be obtained using the Zuber correlation [11]:

$$q''_{chfsat} = 0.131 h_{fg} \left(\sigma g \rho_g^2 (\rho_l - \rho_g)\right)^{0.25} \tag{39}$$

The saturated pool critical heat flux depends on the saturated liquid (ρ_l) and vapour (ρ_g) densities, and the latent heat of evaporation (h_{fg}). If at any point the heat flux from the CT to the bulk fluid exceeds CHF then h_{conv} is assumed to take on the value of the film boiling heat transfer coefficient (h_{fb}). The program makes use of the film boiling heat transfer coefficient described by Gillespie and Moyer [2]:

$$h_{fb} = 0.2(1 + 0.031\Delta T_{sub}) \tag{40}$$

At this point film boiling will be sustained unless the CT temperature drops below the minimum film boiling temperature [11] (T_{mfb}).

$$T_{mfb} = 6.3\Delta T_{sub} + 289 \tag{41}$$

Where $\boldsymbol{\Delta T_{sub}}$ is the degree to which the bulk fluid is subcooled and $\boldsymbol{T_{mfb}}$ is in degrees Celsius.

2.6 Criteria for failure

The current model is limited to the description of average fuel channel behaviour and as such is currently unable to model local necking phenomena that would result in PT/CT failure. Instead the model uses a limiting strain rate of 100%/s as the sole failure criteria. This failure limit is serving as a place holder until a more robust failure limit can be described.

The author would like to acknowledge that Shewfelt et al. [8] described a lower bound failure limit used in the program GRAD that determined the total creep strain required for PT failure ϵ_f.

$$\epsilon_f = -\frac{1}{n} \ln \left\{ 1 - \left[\frac{w_o - d}{w_o} \right]^n \right\} \tag{42}$$

This failure strain was dependent on the initial PT thickness (w_o) and maximum possible defect depth (d) of ~13 μm and the stress exponent (n) of the dominant strain mode ($n = 1.8$ between 450-850°C). This indicates that the PT would fail once it has crept to about 3 times its normal size and would fail at the location of the defect. However, GRAD considered a non-uniform temperature distribution that would develop if the PT was filled to some level with water which would result in a non-uniform creep distribution. That being said this failure limit is exceeded during simulation of SUBC1 and SUBC2 within milliseconds of 100%/s failure limit used in the model since the strain rate rises very rapidly once CT temperatures exceed 600°C.

3. Results

Using the equations outlined in the previous section a model was developed and tested against experimental data provided by Luxat [1]. The experimental test section was composed of a 0.95 m long, 38 mm diameter, graphite heater positioned off centre inside a 1.7 m long section of PT. The PT/heater configuration was isolated from a pool of subcooled water by a 1.75 m long section of CT. Data for 6 combinations of heater linear power, PT internal pressure and degree of pool subcooling (outlined in Table 1) was used to validate the model. Out of the six experiments one (HPCB8) failed due to PT rupture pre-contact and two (SUBC1 & SUBC2) resulted in channel failure due to PT/CT rupture post contact. Figures 3 to 14 at the end of the text compare the PT/CT temperature behaviour obtained experimentally and through simulation.

Table 1 Initial conditions used to test the validity of the designed model.

Test ID	PT Pressure [MPa(g)]	Tank Subcooling [^{o}C]	Heater Power Rating [kW/m]
HPCB2	6.6	29.8	120
HPCB8	10.0	58.0	141
HPCB12	6.5	28.4	135
HPCB13	4.0	19.9	68
SUBC1	3.5	20.0	200
SUBC2	3.5	23.0	195

The model was able to successfully predict fuel channel failure only when the failure occurred post contact (Table 2). The predicted failures times for SUBC1 and SUBC2 fall within seconds of the experimentally observed failure times. The model was unable to successfully predict failure in HPCB8. This model limitation is a direct result of limited failure criteria. PT strain rate will not exceeded 100%/s pre contact and the total strain is restricted to 18% at which point it will make contact with the CT. PT failure before contact is likely a local phenomenon which would require a more robust description of PT strain during heat up in order to be predicted by the model. HPCB8 was also exposed to the highest internal pressure, it is possible that the stress experienced by the PT during heatup exceeded the ultimate tensile strength of Zr-2.5% Nb causing it to fail. Further investigation is underway on predicting pre contact PT failure.

Table 2 Predicted and experimentally observed time to failure with specific failed tube in brackets.

	Time to Failure (s)		
	Experiment	Model	% Difference
HPCB2	--	--	--
HPCB8	84 (PT)	--	--
HPCB12	--	--	--
HPCB13	--	--	--
SUBC1	75 (CT)	74 (CT)	1.33
SUBC2	97 (CT)	95 (CT)	2.06

Focusing on maximum PT and CT temperatures (Table 3 and 4) the PT temperature (excluding HPCB8 which ruptured before contact) are within ~10% of the experimentally observed values. Maximum CT temperature following quenching is underestimated in HPCB13 since the model only allows the convective heat transfer coefficient to be reduced in the event that CHF has been exceeded. The maximum heat flux to the moderator observed in HPCB13 is within 80% of CHF which may be sufficient to temporarily reduce h_{conv} to film boiling conditions. For reference HPCB2, HPCB8, and HPCB12 only come to within 50% of their respective CHF values. That being said short temperature excursions that remain below 600^{o}C, as experienced by HPCB13, would not result in channel failure and the resting PT/CT temperatures remain accurate. For tests where dryout conditions were observed

(SUBC1 and SUBC2) the CT temperatures are over predicted as were the post-contact PT temperatures. This due to significantly reduced, unchanging, film boiling heat transfer coefficient predicted using equation 38. A more robust description of convective heat transfer in all 3 regimes is being investigated.

Table 3 Predicted and experimentally observed maximum PT temperatures.

	Max PT Temp (°C)		
	Experiment	Model	% Difference
HPCB2	730 ± 13	744	1.9
HPCB8	840 ± 60	725	13.7
HPCB12	740 ± 30	749	1.2
HPCB13	750 ± 13	756	0.8
SUBC1	800 ± 30	875	9.4
SUBC2	840 ± 50	874	4.0

Table 4 Predicted and experimentally observed maximum CT temperatures.

	Max CT Temp (°C)		
	Experiment	Model	% Difference
HPCB2	200 ± 115	126	37.0
HPCB8	100 ± 20	125	25.0
HPCB12	160 ± 50	127	20.6
HPCB13	400 ± 20	126	68.5
SUBC1	680 ± 70	816	20.0
SUBC2	700 ± 60	817	16.7

4. Conclusions

Preliminary results are encouraging. Although the model is currently unable to predict short periods of film boiling followed by quench as observed in HPCB13 it is currently able to predict post contact failure within seconds of the experimental results. The CT temperatures predicted by the model in the case of film boiling are over predicted by ~20% of the experimentally observed average and are considered an acceptable conservative estimate. Currently the model is unable to predict PT failure before contact since it is most likely related to local phenomena. Maximum PT temperatures, with the exception of HPCB8, are being correctly predicted within 10% of the average observed temperatures. Further investigation and refinement of CHF, post-dryout film boiling heat transfer coefficient, in addition to pre and post-contact PT/CT failure criteria modelling is underway.

5. References

[1] J. Luxat, "Analysis of High Pressure Contact Boiling Tests," Ontario Power Generation, 2001.

[2] G. Gillespie and R. Moyer, "An Experimental Determination of Heat Transfer from Large Cylinders: Film Boiling in Subcooled Water," AECL, 1984.

[3] R. Shefelt, L. Lyall and D. Godin, "A High Temperature Creep Model for Zr-2.5 wt% Nb Pressure Tubes," *Journal of Nuclear Materials,* pp. 228-235, 1984.

[4] R. Shewfelt and L. L., "A High Temperature Creep Model for Zircaloy-2 Calandria Tubes," COG, 1988.

[5] M. Yovanovich, "New Contact and Gap Conductance Correlations for Conforming Rough Surfaces," in *16th Thermophysics Conference*, Palo Alto, 1981.

[6] Y. L. Shlykov, "Calculating Thermal Contact Conductance Resistance of Machined Metal Surfaces," *Teploenergetika,* vol. 12, pp. 102-108, 1965.

[7] Y. Dai and F. Chiang, "On the Mechanism of Plastic Deformation Induced Surface Roughness," *Journal of Engineering Materials and Technology,* vol. 114, no. 4, pp. 432-438, 1992.

[8] R. Shewfelt and D. Godin, "Verification Tests for GRAD, a Computer Program to Predict the Nonuniform Deformation and Failure of Zr-2.5 wt% Nb Pressure Tubes During a Postulated Loss-of-Coolant Accident," Whiteshell Nuclear Research Establishment, Pinawa, 1985.

[9] H. Rosinger, I. Ritchie and A. Shillinglaw, "Young's Modulus of Crystal Bar Zirconium and Zirconium Alloys (Zircaloy-2, Zircaloy-4, Zirconium-2.5wt% Niobiu,m) to 1000 K," Atomic Energy of Canada Limited, Pinawa, 1975.

[10] A. Mills, Heat Transfer, Upper Saddle River: Prentice-Hall, Inc., 1999.

[11] L. Leung and D. Groeneveld, "Compendium of Thermalhydraulics Correlations and Fluid Properties," COG, 1991.

[12] M. Holmgren, ""X Steam for Matlab"," 2006.

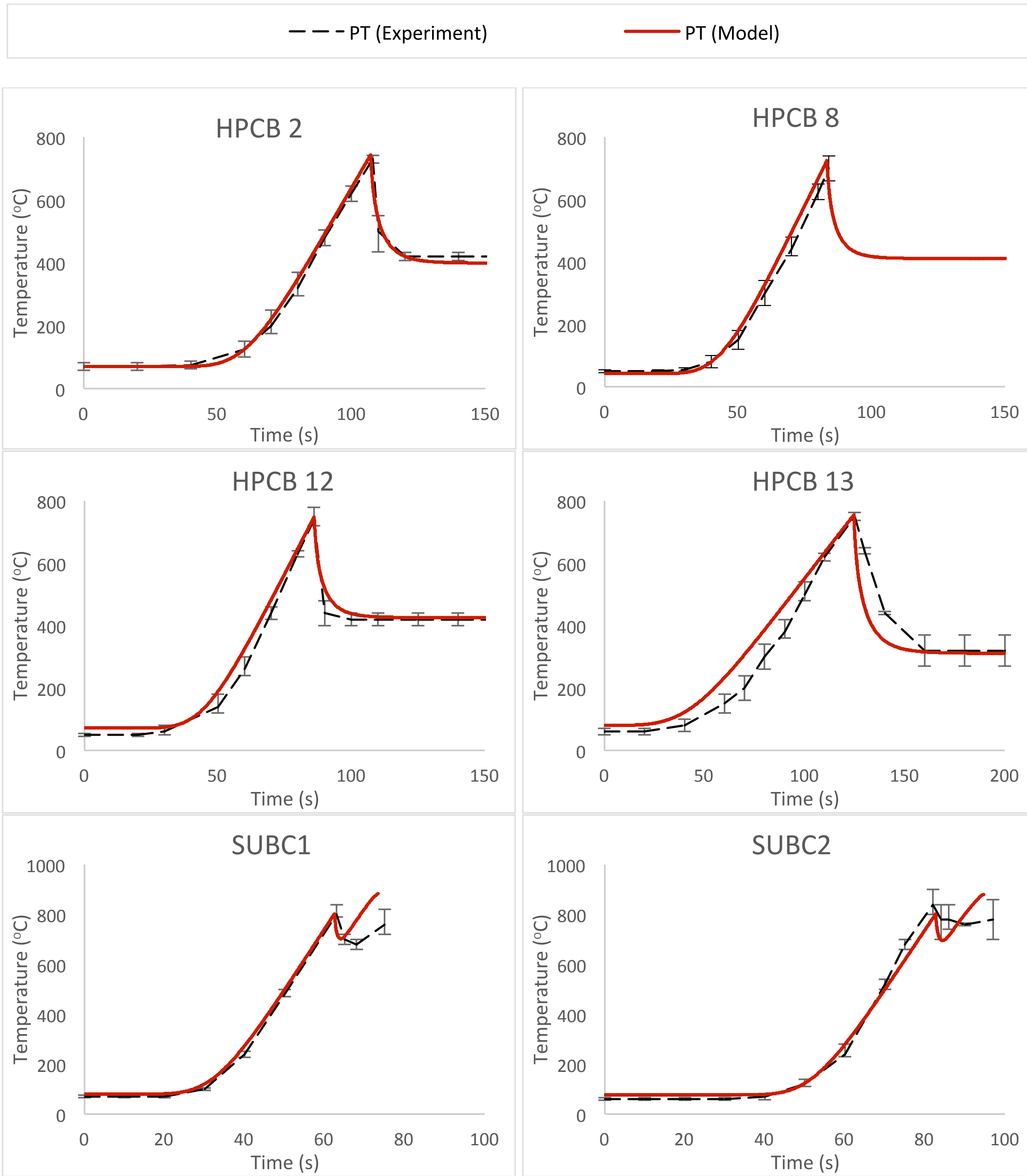

Figure 3-8 Results for predicted temperature behavior (red) of PT during the simulation compared to experimental data (black).

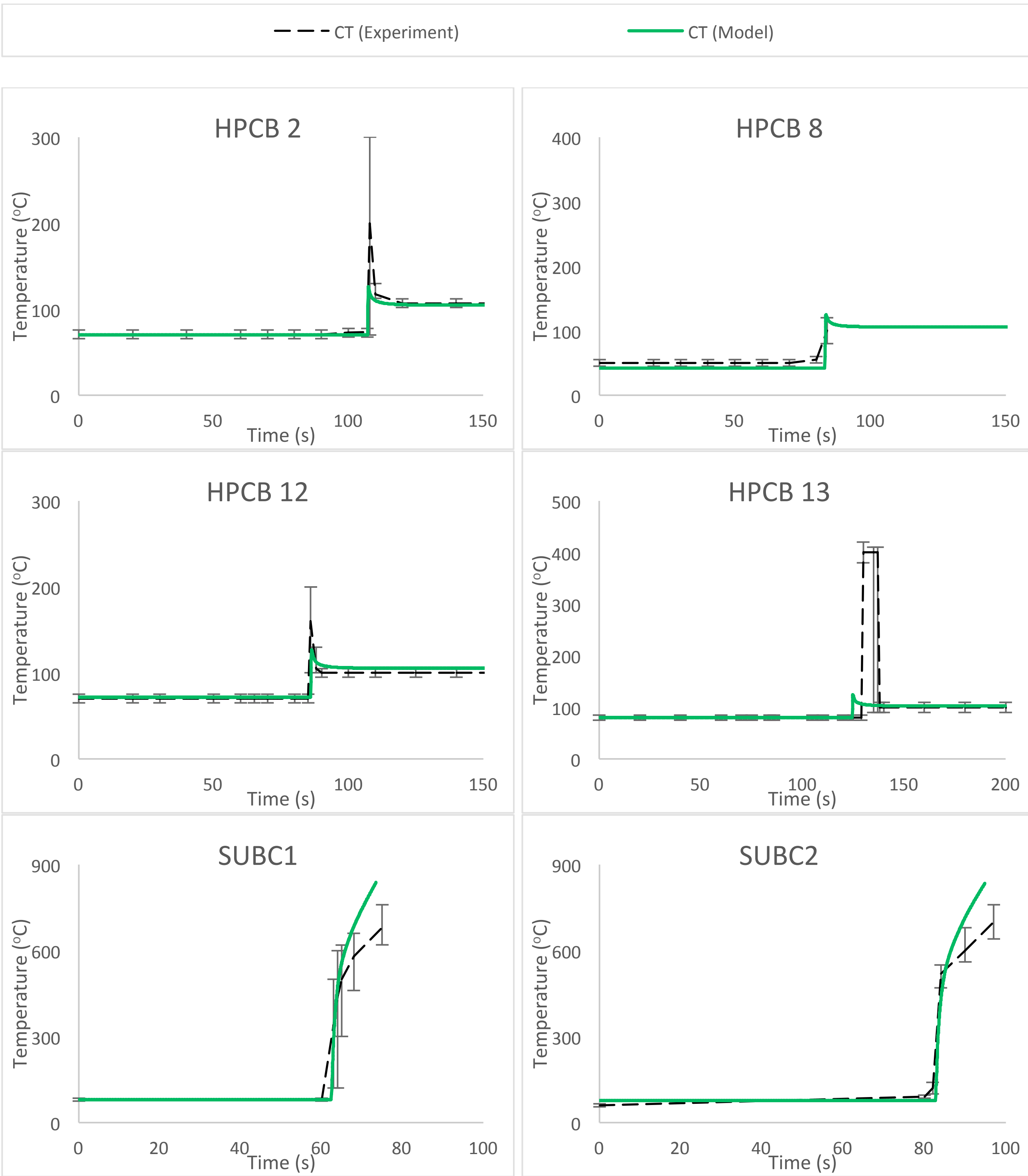

Figure 9-14 Results for predicted temperature behavior (green) of CT during the simulation compared to experimental data (black).